Available online at www.sciencedirect.com
ScienceDirect
Journal of Power Sources 174 (2007) 588–591
JOURNAL OF POWER SOURCES
www.elsevier.com/locate/jpowsour

Short communication

Electrochemical properties of Ni-based inert phases incorporated Si/graphite composite anode

Hansu Kim *, Dongmin Im, Seok Gwang Doo

Energy and Materials Research Lab., Samsung Advanced Institute of Technology, Giheung-Gu, Yong-In City, Republic of Korea

Available online 27 June 2007

Abstract

Ni-based inert phases incorporated Si/graphite composite, prepared by thermal decomposition of a mixture of nickel stearate and Si/graphite composite, was investigated as an anode material for lithium-ion batteries. The first discharge and charge capacities of this material were 940 and 640 mAh g^{-1}, respectively, with 72% of the first cycle coulombic efficiency. Back scattered electron image of the cross section of this material revealed that Ni-based inert phases, i.e., Ni and Ni_2Si were finely dispersed in the Si/graphite matrix. Ex situ X-ray diffraction results indicated that those Ni-based inert phases were inactive against lithium, and they are believed to improve the electrical conduction network inside the active material and to alleviate to some extent the mechanical stresses associated with volume changes during cycling.

Keywords: Lithium; Battery; Anode; Silicon; Mechanical alloying; Si/C nanocomposite

1. Introduction

Silicon-based anode material has attracted much interest as an alternative for graphite anode in lithium-ion batteries as it provides high energy density. However, a major drawback of this material is its poor cyclability associated with a large volume change during the alloying/dealloying reaction of Si with Li. One of the ways to improve the cyclability of silicon-based anode is the use of active/inactive phase composite to alleviate the influence of Si expansion and to preserve the structural integrity by the introduction of buffer matrix which is electrochemically less active than Si or inactive and has good electrical conductivity. Carbonaceous materials, such as graphite and disordered carbon, have been investigated intensively as the buffer matrix phase and those Si/carbon composites have been found to show improved cyclability compared with Si [1–4]. In an attempt to enhance the capacity retention of Si/carbon composites, many research groups have focused on the modification with transition metal or metal–silicon alloy which acts as an inert phase to lessen the mechanical stresses and preserve the electrical pathways in the active material [5–9]. In this work, we have prepared a Ni-based inert phases incorporated Si/graphite composite using a simple thermal decomposition of a mixture of nickel stearate and a high energy ball-milled Si/graphite composite and investigated it as the anode material for lithium-ion batteries.

2. Experimental

Si/graphite composite was prepared by the following procedure. Si (99.99%, Noah, USA) and graphite (SFG-6, Timcal) powders with a weight ratio of 1:2 were put into a stainless steel vial with hardened steel balls at a ball to powder ratio of 7:1 by weight. The vial, assembled under Ar atmosphere, was installed on SPEX-8000M mixer/mill and the mixture was milled for 1 h.

The Ni-based inert phases incorporated Si/graphite composite was prepared by the following procedure. The Si/graphite composite and nickel stearate (Strem chemical) with a molar ratio (Ni/Si) of 0.2 were homogeneously blended in a mortar and then heated at 120 °C for the melting of nickel stearate. The mixture, i.e., Si/graphite composite powder with melted nickel stearate, was cooled down to room temperature and mixed again for homogeneous blending, followed by a pyrolysis carried out at 900 °C for 1 h under Ar atmosphere.

The electrodes were prepared by coating the slurries (active material powder (75 wt.%), graphite powder (SFG-6) (15 wt.%), and polyvinylidene fluoride (PVDF) as a binder (10 wt.%) dissolved in *n*-methyl pyrrolidinone (NMP)) on a Cu foil substrate.

* Corresponding author. Tel.: +82 31 280 9395; fax: +81 31 280 9359.
E-mail address: khansu@samsung.com (H. Kim).

0378-7753/$ – see front matter © 2007 Elsevier B.V. All rights reserved.
doi:10.1016/j.jpowsour.2007.06.121

After the coating, the electrodes were pressed and dried for 2 h at 120 °C under vacuum. The electrodes were cut into disks (13 mm in diameter and about 0.06 mm in thickness) and mass of active material in a disk electrode was approximately 3 mg. Coin type cells (CR2016) were assembled in a dry room using Celgard 3501 as separator, 1.3 M $LiPF_6$, ethylene carbonate (EC)/diethyl carbonate (DEC) (3:7 vol.%, Cheil Industries, Korea) as electrolyte, and Li foils as counter and reference electrodes. All cells were tested at a constant current of 100 mAh g^{-1} within a fixed voltage window (0.001–1.5 V).

Synthesized materials were characterized using an X-ray diffractometer (XRD, Rigaku, RINT2200HF+), a Raman spectrometer (Renishaw, Raman system 3000) and a field emission scanning electron microscope (FE-SEM, Hitachi, S-4200) attached with energy dispersive (EDS) X-ray analyser (EDAX® GENESIS4000). To record the ex situ XRD patterns of the electrodes removed from the tested cells, Kapton films were used to protect the electrodes from aerial oxidation.

3. Results and discussion

Fig. 1 shows the XRD patterns of the mechanically milled Si/graphite composite, the pyrolysis product of the mixture of nickel stearate and the Si/graphite composite at 900 °C, and a Ni/C composite prepared by a pyrolysis of nickel stearate only at the same temperature. Fig. 1(b) and (c) shows the presence of Si and graphite in the mechanically milled Si/graphite composite and heat treated milled Si/graphite composite with nickel stearate. It should be noted that the interlayer spacing (d_{002}) corresponding to the graphite in these composites was 3.36 Å, which is the same as that of unmilled starting material, graphite (SFG-6). It indicates that the highly ordered graphene layer in the composites did not collapse after mechanical milling and heat treatment. However, it was observed that the line broadening in the XRD patterns of these composites, which was probably due to the decrease of the crystallite size and the increase of the internal strain induced by mechanical milling. These results imply that graphite in the milled Si/graphite composite retained its crystal structure with the increased defects after milling and the heat treatment at 900 °C.

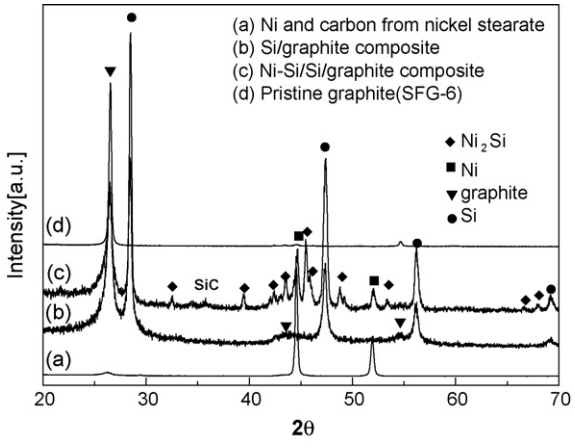

Fig. 1. XRD patterns of (a) pyrolyzed nickel stearate, (b) ball-milled Si/graphite composite, (c) the product obtained from the pyrolysis of the mixture of nickel stearate and Si/graphite composite, and (d) pristine graphite (SFG-6).

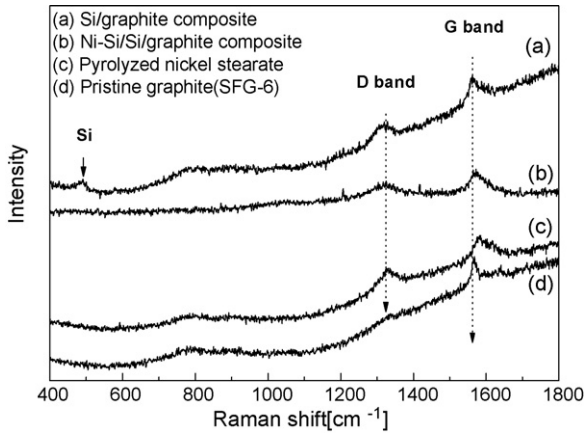

Fig. 2. Raman spectra of (a) ball-milled Si/graphite composite, (b) the product obtained from the pyrolysis of the mixture of nickel stearate and Si/graphite composite, (c) pyrolyzed nickel stearate, and (d) pristine graphite (SFG-6).

Metallic Ni with carbon is obtained from the thermal decomposition of nickel stearate at 900 °C, which is in well accordance with the report of Geng et al. [10] on a direct conversion of nickel stearate into Ni nanoparticles covered with carbonaceous materials. It is noted in the pattern (c) that Ni-based inert phases, i.e., Ni_2Si and Ni, can be incorporated into the Si/graphite composite by such simple processes: mixing of nickel stearate with the Si/graphite composite and a heat treatment. The formation of Ni_2Si is probably due to the reaction of Si dispersed in the Si/graphite composite with a part of Ni from the nickel stearate during the heat treatment.

Raman spectra of Si/graphite composite, Ni-based inert phases incorporated Si/graphite composite, and the pyrolysis product of nickel stearate are presented in Fig. 2. It was observed in the milled composites and pyrolyzed nickel stearate that G-band and D-band, representing graphitic carbon and disordered carbon, respectively [11], while unmilled graphite exhibits only G-band at 1580 cm^{-1}, indicating that mechanical milling increased the defects of the graphite. It should be noted that the Raman shift corresponding to Si at 520 cm^{-1} in the Si/graphite composite (Fig. 2(c)) disappears in the spectrum of Ni_2Si–Ni incorporated Si/graphite composite (Fig. 2(b)). Considering Raman spectroscopy is a surface sensitive analytical technique, it is believed that Si on the surface of the Si/graphite composite has completely reacted with Ni forming Ni_2Si during the heat treatment.

Elemental composition of the composites with the help of EDS analysis is presented in Table 1. Iron contamination from the milling media could not be observed.

Table 1
Elemental composition of Si/carbon composite and the product obtained from the pyrolysis of the mixture of nickel stearate and Si/graphite composite

	C (wt%)	Si (wt%)	Ni (wt%)
Si/graphite composite	69.11	30.89	
Ni–Si/Si/graphite composite	70.24	20.24	9.52

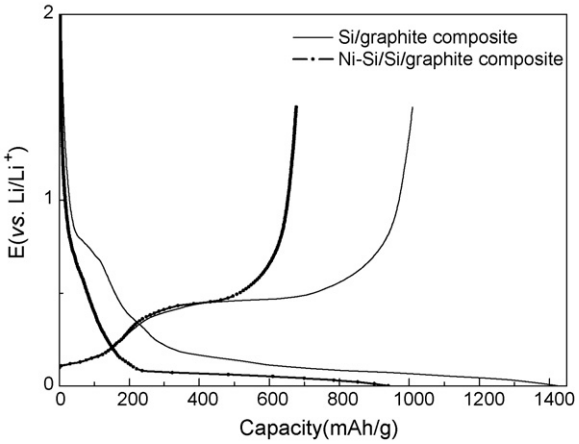

Fig. 3. Voltage profile of Si/graphite composite (thin line) and Ni-based inert phase incorporated Si/graphite composite (thick line) for the first cycle.

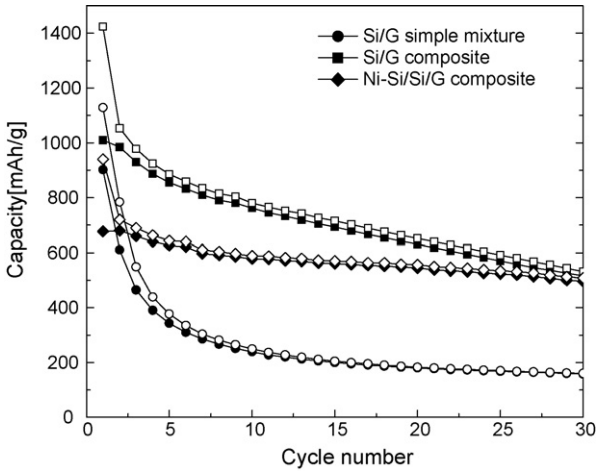

Fig. 4. Cycle life performance of Si/graphite simple mixture electrode, Si/graphite composite electrode and Ni-based inert phases added Si/graphite composite electrode cycled between 0.0 and 1.5 V (vs. Li/Li^+).

Fig. 3 shows the voltage profiles of the electrodes made of Si/graphite composite and Ni_2Si–Ni incorporated Si/graphite composite for the first cycle. Discharge (lithiation) and charge (de-lithiation) capacity of the Si/graphite composite electrode is 1423 and 1009 mAh g^{-1}, respectively. Taking into account the capacity and the proportion of the conductive agent in the electrode, which is 360 mAh g^{-1} and 16.6%, respectively, the discharge and charge capacity of milled Si/graphite composite is 1636 and 1139 mAh g^{-1}, respectively. The coulombic efficiency in the first cycle is 70.9%. The irreversible capacity is probably due to the electrolyte decomposition on the surface of active material during the first lithiation, especially on the surface of the disordered carbon formed and dangling bond on the surface of the milled silicon during the high energy mechanical milling of graphite [12]. Discharge and charge capacity of Ni-based inert phases incorporated Si/graphite electrode is 940 (discharge) and 680 mAh g^{-1} (charge), respectively. Calculated discharge and charge capacity of this composite is 1056 and 744 mAh g^{-1}, respectively. The first cycle efficiency is 72.3%, which is slightly better than that of Si/graphite composite.

As shown in Fig. 3, the sloping potential plateau around 0.8 V (versus Li/Li^+) in the lithiation of the Si/graphite composite electrode, which is well known as the outcome of electrolyte decomposition and solid electrolyte interface formation, is significantly reduced in the discharge voltage profile of Ni-based inert phases incorporated Si/graphite composite electrode. This small increase in the coulombic efficiency is possibly due to the presence of carbonaceous material formed in the thermal decomposition process of nickel stearate, which might be covering the surfaces of disordered carbon in the high energy milled Si/graphite composite and consequently reduce the irreversible electrolyte decomposition reaction [5,14].

Notwithstanding the improved coulombic efficiency, Ni-based inert phases incorporated Si/graphite composite shows a less charge/discharge capacity compared to the Si/graphite composite. It is attributed to the decrease in the weight fraction of electrochemically active Si since a part of Si has been consumed by the formation of Ni_2Si and SiC. And Ni, an inert element and carbon, less active than Si from thermal decomposition of nickel stearate, has been incorporated as well.

Fig. 4 shows the capacity retention of Ni-based inert phases incorporated composite is considerably enhanced compared with the raw Si/graphite composite. The reason for the enhanced cyclability may be attributed to the electrically conductive and also inactive phases in the active material, i.e., Ni_2Si and nickel. Fig. 5 shows ex situ XRD patterns of the Ni-based inert phases incorporated composite electrodes in the first lithiation/de-lithiation cycle. When the electrode is fully lithiated up to 1 mV (versus Li/Li^+), the peaks corresponding to Si disappears and $Li_{15}Si_4$ peaks emerge instead [13]. In other hand, Ni and Ni_2Si peaks are intact even after the full lithiation and the subsequent de-lithiation, indicating that Ni and Ni_2Si act as the phases inert to lithium during cycling as expected.

The FE-SEM photographs in Fig. 6 are the back scattered electron (BSE) images showing the cross-section of Si/graphite composite (Fig. 6(a)) and Ni_2Si–Ni incorporated Si/graphite composite (Fig. 6(b)), respectively, in which the elements can be discerned by contrast: regions with heavier element are brighter.

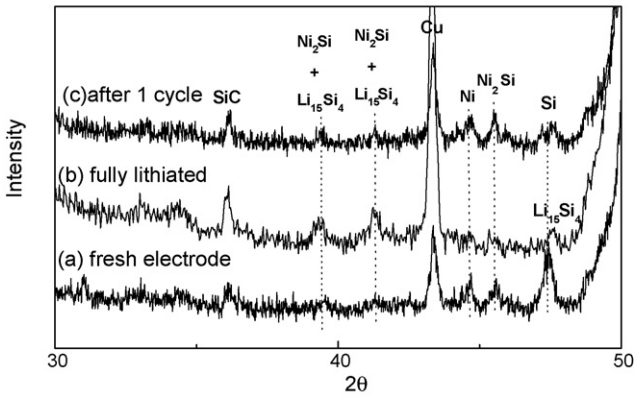

Fig. 5. XRD patterns of (a) fresh electrode, (b) fully lithiated electrode, and (c) the electrode after the first cycle.

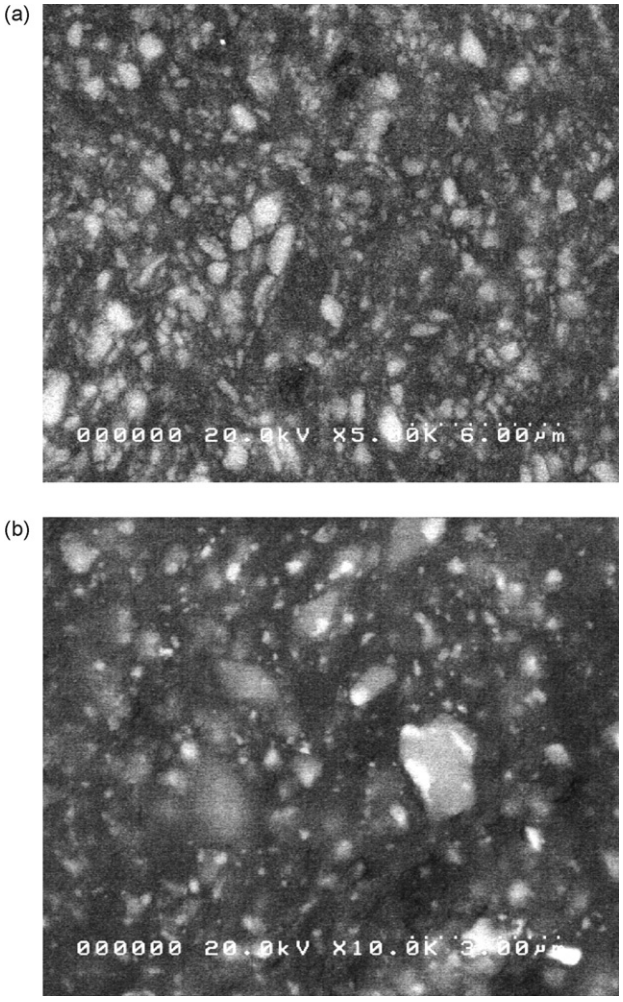

Fig. 6. Back scattered electron images of the cross section of (a) Si/graphite composite and (b) Ni-based inert phases added Si/graphite composite.

Fig. 6(a) confirms the presence of two different phases, i.e., Si and graphite, in the Si/graphite composite. Si particles distinguished as white spots in the BSE image are finely dispersed in the graphite matrix and the size of them from 0.1 to 2 μm. In the Ni_2Si–Ni incorporated Si/graphite composite (Fig. 6(b)), on the other hand, at least three different elements can be clearly recognized. The brightest regions reflecting Ni are finely dispersed in the Si/graphite composite. Most of them are located near Si particles (the medium contrast regions) and some of Ni-rich regions are overlapped with Si particles, indicating that Ni_2Si adheres onto Si particles. The formation of Ni_2Si phase might have reduced the size of pure Si in the active material, accounting for the decreased specific capacity. However, Ni_2Si on the surface of Si particles might provide better electrical connection between electrochemically active Si phase and graphite matrix even if a mechanical stress is accumulated at the interface upon the repeated expansion/contraction of Si phase during cycling.

4. Conclusions

Ni-based inert phases incorporated Si/graphite composite was prepared via a thermal decomposition of a mixture of nickel stearate and a mechanically milled Si/graphite composite. Improved capacity retention could be achieved compared with unmodified Si/graphite composite. Ex situ XRD results and BSE images of the composites showed Ni-based inert phases were finely incorporated into the active material and electrochemically inactive against lithium. The improved cyclability of this material could be attributed to finely dispersed electrically conducting inactive phases of Ni and Ni_2Si.

References

[1] M. Yoshio, H. Wang, K. Fukuda, T. Umeno, N. Dimov, Z. Ogumi, J. Electrochem. Soc. 149 (2002) A1598.
[2] I.-S. Kim, P.N. Kumta, J. Power Sources 136 (2004) 145.
[3] G.X. Wang, J.H. Ahn, J. Yao, S. Bewlay, H.K. Liu, Electrochem. Commun. 6 (2004) 689.
[4] Y. Liu, K. Hanai, J. Yang, N. Imanishi, A. Hirano, Y. Takeda, Electrochem. Solid State Lett. 7 (2004) A369.
[5] H.-Y. Lee, Y.-L. Kim, M.K. Hong, S.-M. Lee, J. Power Sources 141 (2005) 159.
[6] B.-C. Kim, H. Uono, T. Satou, T. Fuse, T. Ishihara, M. Ue, M. Senna, J. Electrochem. Soc. 152 (2005) A523.
[7] J.-H. Kim, H. Kim, H.-J. Sohn, Electrochem. Commun. 7 (2004) 557.
[8] M.S. Park, Y.J. Lee, S. Rajendran, M.S. Song, H.S. Kim, J.Y. Lee, Electrochim. Acta 50 (2005) 5561.
[9] T. Kim, S. Park, S.M. Oh, Electrochem. Commun. 8 (2006) 1461.
[10] J. Geng, D. Jefferson, B.F.G. Johnson, J. Mater. Chem. 15 (2005) 844.
[11] Y. Kawashima, G. Katagiri, Phys. Rev. B 52 (1995) 10053.
[12] Y. Liu, K. Hanai, K. Horikawa, N. Imanishi, A. Hirano, Y. Takeda, Mater. Chem. Phys. 89 (2005) 80.
[13] M.N. Obrovac, L. Christensen, Electrochem. Solid State Lett. 7 (2004) A93.
[14] H.-Y. Lee, S.-M. Lee, Electrochem. Commun. 6 (2004) 465.